Performance Degradation of Propeller Systems Due to Rime Ice Accretion

K. D. Korkan*
Texas A&M University, College Station, Texas
and
L. Dadone†
Boeing Vertol Company. Philadelphia, Pennsylvania
and
R. J. Shaw‡
NASA Lewis Research Center, Cleveland, Ohio

A theoretical ice accretion model has been established applicable to both aircraft propellers and helicopter rotors to determine the effect of rime ice on the thrust, power, and efficiency as a function of exposure time in a natural icing condition. Comparisons have been made of theoretical performance levels with previously published experimentally determined propeller thrust and efficiency for five natural icing conditions. Agreement between test and theory was acceptable.

Nomenclature

A_c = accumulation parameter = $U(\text{LWC})\Delta t/\rho_{\text{ice}} c$
b,c = airfoil chord
C_D = drag coefficient = $D/q_\infty c$
C_L = lift coefficient = $L/q_\infty c$
C_p = power coefficient = $P/\rho n^3 D^5$
C_T = thrust coefficient = $T/\rho n^2 D^4$
D = diameter
E = collection efficiency
h,t = blade thickness
I = drag constant, Eq. (1)
J = advance ratio = V/nD
k/c = roughness height, Eq. (1)
LWC = liquid water content
n = revolutions per second
q_∞ = freestream dynamic pressure = $\frac{1}{2}\rho_\infty V_\infty^2$
r = local radius
R = radius
V_i = induced velocity
V_∞, U = freestream velocity
x = airfoil chord location
y = airfoil thickness location
α = angle of attack
β = blade twist angle; droplet impingement efficiency
$\beta_{\max}$ = maximum droplet impingement efficiency
Δt = icing time
η = propeller efficiency = $(C_T/C_p)/J$
ρ_{ice} = ice density
ρ_∞ = freestream density

Introduction

PREVIOUS investigations[1-5] of propeller characteristics during natural icing conditions indicate significant performance degradation. For example, Preston and Blackman[6] undertook a flight test investigation to determine the effect of ice formations on propellers, wing, empennage, engine cowlings, and miscellaneous unprotected components on aircraft performance in level cruising flight. The authors reported a maximum loss of 19% in propeller efficiency ($\Delta\eta$) due to ice formation. Also, during 87% of the propeller icing encounters, efficiency losses of approximately 10% were observed. In a later study by Neel and Bright,[7] flight records were compiled for natural icing conditions over commercial routes. Neel and Bright allowed ice to form on the propeller of the right engine, with the left engine being kept clear on a two-engine aircraft. Ice accumulation was measured with thickness varying from zero to 1 in. Also, the spanwise extent of icing, measured in percent of blade radius, varied from zero to 95%. With this type of icing, maximum losses in efficiency of up to 20% were encountered, thereby severely compromising the performance of the aircraft. Work is continuing in the field of propeller icing, as noted by Sweet,[8] who also verified efficiency degradation levels on the order of from 10 to 20%.

The ice shapes found on fixed wing configurations can be classified into two categories, i.e., rime and glaze, each having distinct physical characteristics. Examples of the rime ice condition on a propeller have been experimentally found, as shown in Fig. 1 (Ref. 9). Here, the ice accretion has taken place along the entire span of the propeller blade, with no evidence of shedding. However, in the same series of tests under different meteorological conditions,[9] glaze ice was also encountered outboard of the de-ice boot in addition to shedding (Fig. 2).[9]

Theoretical icing models do exist for fixed wing configurations. However, to determine the ice buildup on existing propeller-nacelle-aircraft configurations, tests are typically carried out by flying in the wake of an icing tanker or seeking out a natural icing encounter. That is, icing considerations are of importance only after the requirements for nonicing performance are satisfied. Discussions with various propeller manufacturers showed that a propeller is selected to meet the specific requirements of an aircraft/engine combination. Consideration is then given to determine the type and extent of icing protection. Ice is allowed to build up along the propeller blade until such time when the de-ice boots are energized to reduce the force of adhesion between the ice and

Presented as Paper 82-0286 at the AIAA 20th Aerospace Sciences Meeting, Orlando, Florida, Jan. 11-14, 1982; submitted April 19, 1982; revision received Sept. 11, 1983.

*Associate Professor, Aerospace Engineering Department.
†Engineering Specialist, Aerodynamics Department.
‡Aerospace Scientist, Icing Research Section.

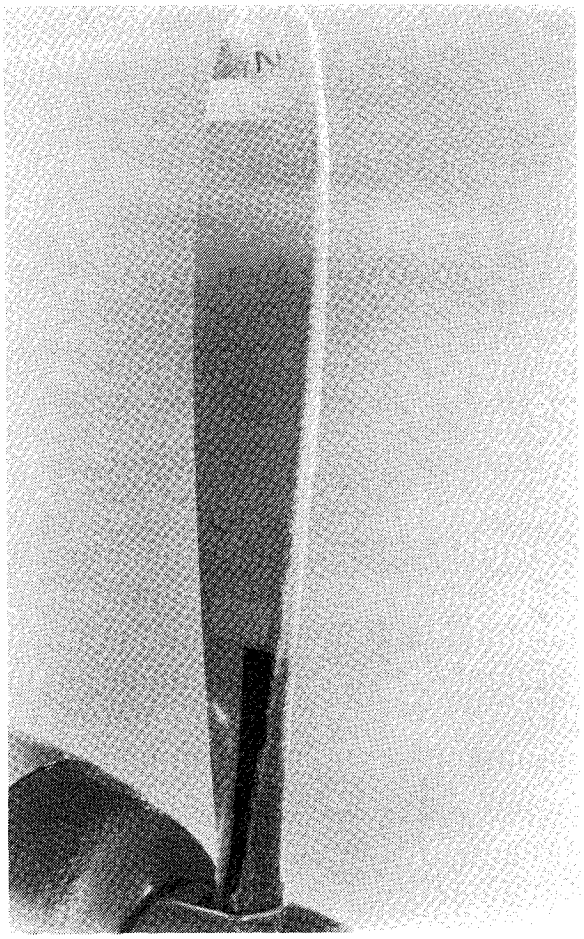

Fig. 1 Rime ice accretion on propeller blade (Ref. 9).

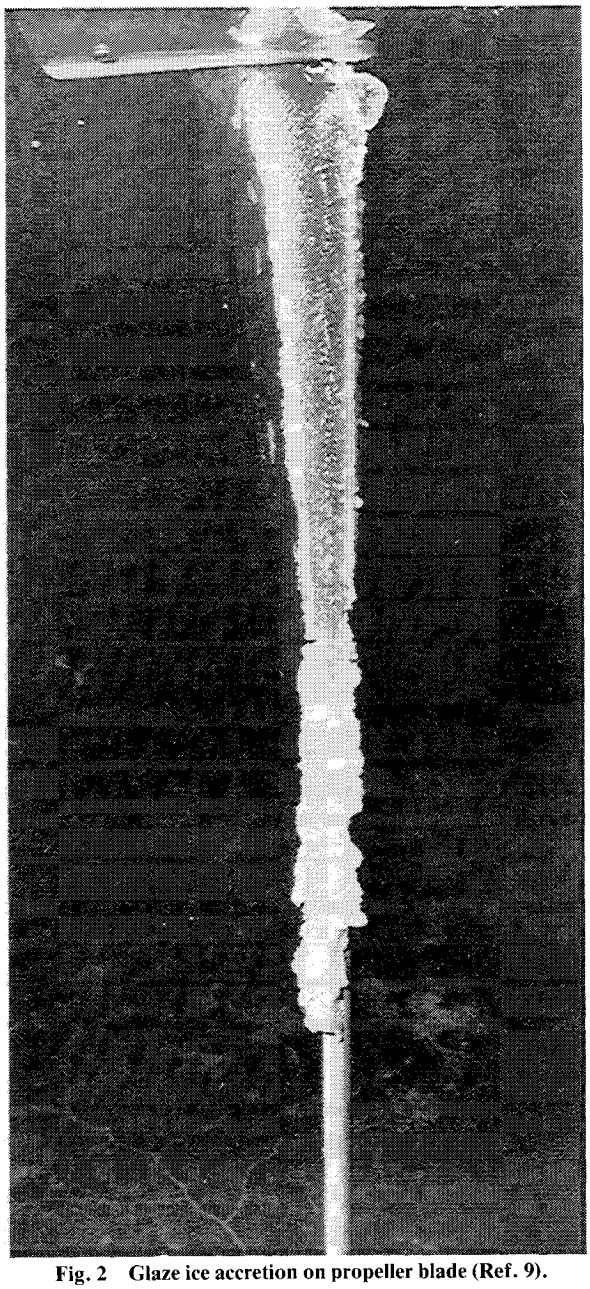

Fig. 2 Glaze ice accretion on propeller blade (Ref. 9).

the boot. Centrifugal force then removes the ice, the de-icing system is deactivated, and the cycle is repeated.

The study objectives of the present effort were to establish a theoretical methodology to predict the performance degradation of propellers in a natural icing encounter. Only the rime ice accretion case was considered to determine its effects on the propeller thrust coefficient, power coefficient, and efficiency as a function of time.

Method of Analysis

The first step in the present study was the development of a two-dimensional theoretical icing model applicable to propellers. As indicated in Fig. 3, the propeller flowfield with rotating airfoil sections encounters not only the forward but also rotational and induced velocity components. These velocity components determine the resultant velocity and the effective pitch angle, hence the angle of attack, as seen by each airfoil section along the propeller blade. Here, the angle of attack is taken as the difference between the geometric pitch angle and effective pitch angle and includes the induced velocity component at each station along the propeller blade.

The flowfield encountered by the rotating airfoil section in the disk plane, when considering only the resultant velocity vector (Fig. 3), does not differ to a great extent from that of a "wing airfoil." However, the application of the theoretical model of Bragg et. al.[10,11] to the propeller icing problem does require a different set of initial conditions for the water droplet trajectories. In the propeller case, the droplet is started at the freestream velocity V_∞ and allowed to progress toward the disk plane. However, superimposed upon the V_∞ component will be an induced velocity component, which is $V_i = 0$ far upstream of the disk plane and increases to V_i at the disk plane. Therefore the water droplet, upon entering the disk plane, goes from the $V_\infty + V_i$ velocity component to the resultant velocity vector, which determines the droplet trajectory and possible impingement on the propeller airfoil section. Since the local induced velocity is a function of the propeller radial location, each airfoil section must be treated separately as to this boundary condition and the radial variation of the local Mach number and local angle of attack (Fig. 4).

The airfoil icing analysis of Bragg et. al.[10,11] used in this study has been formulated to predict the fixed, i.e., non-rotating airfoil performance degradation due to ice accretion. A Theodorsen transformation method is used to calculate the inviscid flowfield around the airfoil. This flowfield is then used to compute, by step integration, the trajectories of the water droplets and the location of impingement of the water droplet on the airfoil surface. This information is utilized to predict the local impingement efficiency and accumulation parameter on the airfoil surface. The method of Bragg et. al.[10,11] is directly applicable to the study of propeller icing by taking into account the new boundary conditions previously described at specific radial locations along the propeller. Also note that this study, as does the method of Bragg, assumes the rime ice case, i.e., that the entire mass of the water droplets

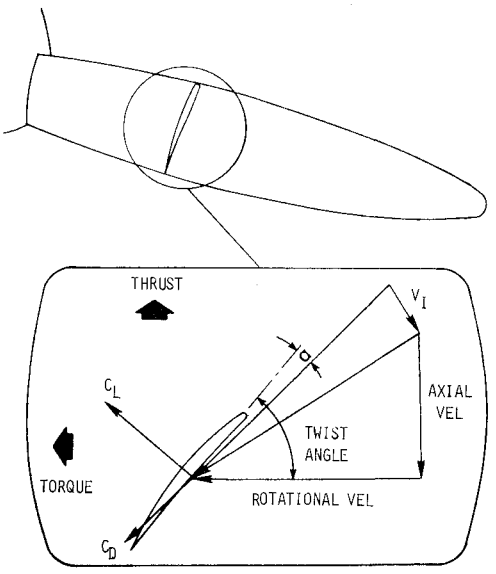

Fig. 3 Velocity components about a two-dimensional propeller section.

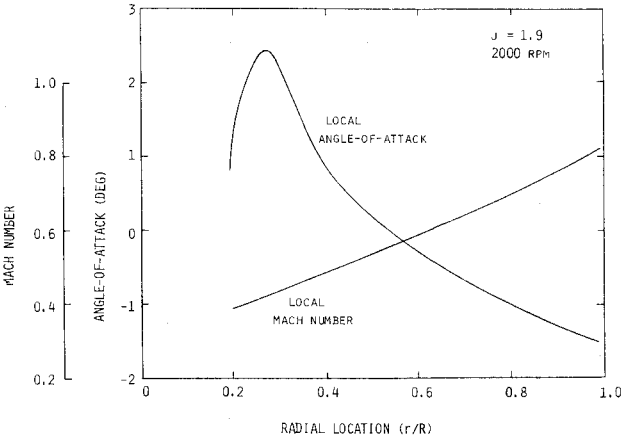

Fig. 4 Variation of local angle of attack and Mach number as a function of propeller radius (J, rpm, β constant).

freezes on contact at the point of impact, and that no thermodynamic effects have been included.

The analytical method then consists of the following steps:

1) An existing propeller performance method[12] is used to obtain the local Mach number and angle of attack (Fig. 4) as a function of radial location along the propeller for the nonice condition at a preselected operating condition. The reader is referred to a review of performance methodologies by Korkan et. al.[13,14]

2) Select a volume median droplet diameter. Through a previous study by Bragg and Gregorek,[10] it has been shown that by appropriate selection of a volume median droplet diameter, the entire class of droplet diameters encountered need not be considered.

3) Select the liquid water content to considered.

4) Using the Theodorsen transformation method, calculate and store the inviscid flowfield around each airfoil station at the given angle of attack for each radial location along the propeller for the operating condition of interest.

5) Calculate the water droplet trajectories using the volume median droplet diameter in step 2 for each airfoil along the propeller.

6) Determine the impingement efficiency and accumulation parameter for each airfoil station along the propeller.

7) Calculate the drag increment for each airfoil station at the specified icing time and operating condition. The airfoil

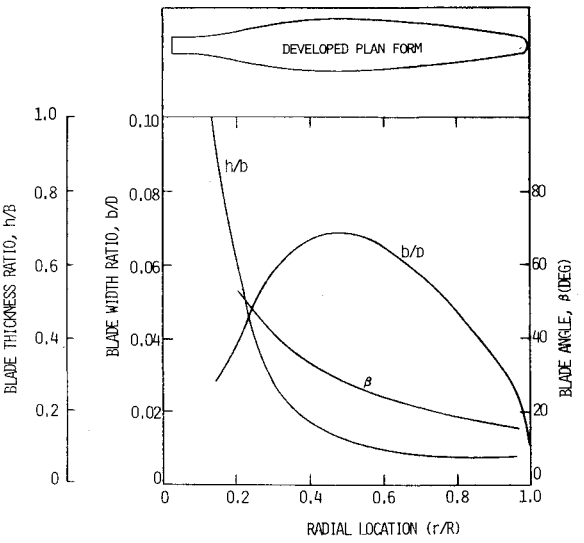

Fig. 5 Characteristics of test propeller.

data bank for performance analysis is then modified by applying the $(1 + \Delta C_D/C_D)$ factor.

The propeller performance analysis[12] is finally utilized to determine the performance degradation on the basis of η, C_T, and C_p at the operating condition of interest.

In the calculation of the drag increment due to ice accretion, the empirical correlation of Bragg and Gregorek[11] was used directly, with no modification to the constants, i.e.,

$$\frac{\Delta C_D}{C_D} = 0.010[15.798\ln(\frac{k}{c}) + 28{,}000A_cE + I] \quad (1)$$

This empirical correlation includes the drag increment related to the distortion of the airfoil leading edge due to rime ice accretion and a step drag increase based on surface roughness data. The contant I is dependent on airfoil type and ranges from 184 to 290.

The new drag of the airfoil in the icing condition and hence the modified data bank may be obtained from the expression

$$C_{D_{\text{ice}}} = (1 + \Delta C_D/C_D)\, C_D \quad (2)$$

where the C_D value is for the no-ice condition and is contained in the airfoil data bank as used by the propeller performance analysis or can be determined by existing airfoil analyses methods and/or experiment. The above drag correlation is only valid for the rime ice condition.

Experimental/Theoretical Comparisons of Propeller Performance in a Natural Icing Encounter

The analytical model just described was utilized to provide theoretical predictions of propeller performance degradation for comparison with experimental flight test results by Neel and Bright.[7] Here, the authors conducted a series of flight tests with a C-46 twin-engine aircraft. The test propeller, having a diameter of 13.5 ft, consisted of four blades utilizing double camber Clark Y airfoil sections. Characteristics of the blade design, supplied by the manufacturer, are given in Fig. 5. A thrust meter and torquemeter were installed on the right engine shaft to measure the thrust and torque absorbed by the propeller. Calibration of the thrust meter indicated an accuracy of $\pm 1\%$ of maximum thrust through a wide range of propeller thrust levels. No special calibration of the torquemeter was made, with the exception of verifying the repeatability of measurements for a fixed operating condition in a no-ice condition. The authors stated that the propeller efficiency was repeatable within $\pm 2\%$. The reader is referred to Ref. 7 for the details of the flight test.

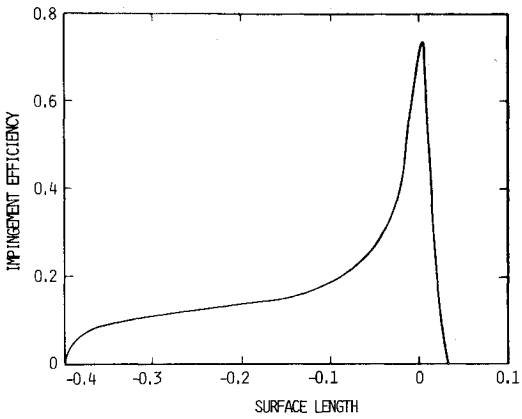

Fig. 6 Example of impingement efficiency variation vs airfoil surface length-encounter 2, $r/R = 0.975$, $J = 1.2$, $\alpha = 4.624$ deg.

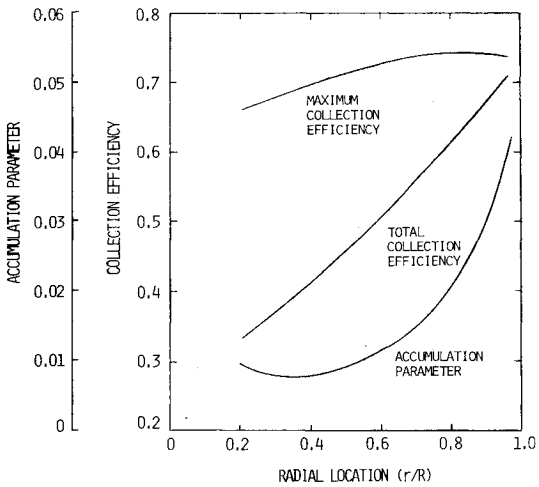

Fig. 7 Variation of accumulation parameter, total collection efficiency, and maximum collection efficiency as a function of radial location-encounter 2, $J = 1.2$.

A series of 12 encounters was examined by Neel and Bright.[7] The test procedure consisted of obtaining base line performance data in clear air. Natural icing conditions were then sought and ice accretion allowed to take place on the test propeller while, at the same time, applying heat to the wings, tail, windshield, and left propeller. Simultaneously, liquid water content, droplet size, and free air temperature were measured. Upon completion of the ice accretion process, the propeller blade angle was set, and measurements were made of airspeed, altitude, and rotational speed, thrust, and torque of the test propeller. Of the 12 encounters,[7] five were chosen for comparison with the analytical model of rime ice accretion based on free air temperature, average liquid water content, and the average droplet diameter, as shown in Table 1.

The theoretical methodology described earlier, when applied to encounter 2 with a fixed J value, yields a trend in impingement efficiency variation as a function of airfoil surface length for each radial station along the propeller. Figure 6 shows a typical β variation for r/R of 0.975 and also indicates βmax. The total collection efficiency, maximum collection efficiency, and the accumulation parameter[10] defined by

$$A_c = U(\mathrm{LWC})\,\Delta t/\rho_{\mathrm{ice}} c \qquad (3)$$

are then determined for all radial locations along the propeller blade, as shown in Fig. 7. Next, these values are used in the drag coefficient correlation as given in Eq. (1) to determine

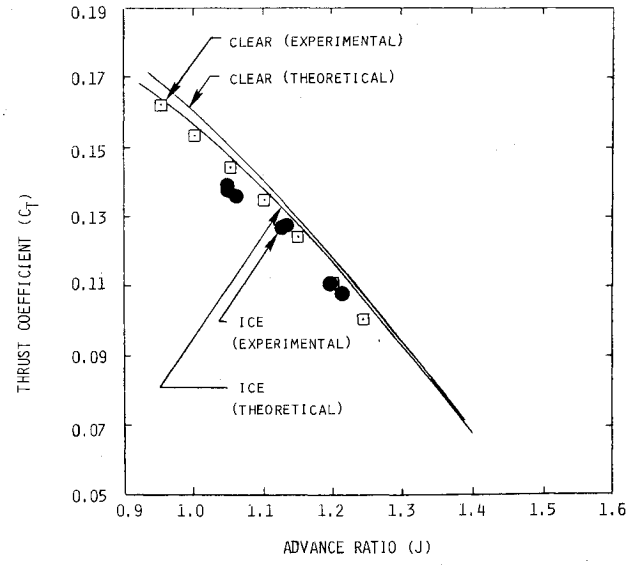

Fig. 8 Comparison between theoretical/experimental C_T values —encounter 2 (Ref. 7).

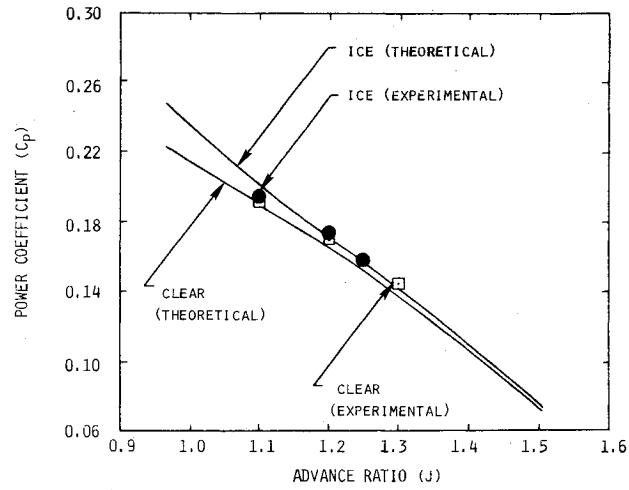

Fig. 9 Comparison between theoretical/experimental C_p values — encounter 2 (Ref. 7).

the appropriate $\Delta C_D/C_D$ values for the basic two-dimensional airfoil sectional characteristics as used in the propeller performance method.[12] Comparisons for encounter 2 between the experimental values and the theoretical predictions are shown in Figs. 8-10. It may be seen that the theoretical thrust coefficient values are generally higher than the experimental values and are related to excluding the decambering effect due to ice accretion at the leading edge of the airfoil, resulting in a shift in the zero lift angle of attack. However, the incremental reduction in C_T due to ice is consistent with the measured experimental values. The iced condition also results in an increase in C_p values, since C_p is related to the torque coefficient and hence the drag of each of the airfoil sections. For the propeller efficiency η, the agreement between theoretical predictions and experiment for both iced and clear conditions is acceptable as shown in Fig. 10. Similar agreement was found for all the icing encounters considered, as shown in Fig. 11 (encounter 4) and Fig. 12 (encounter 12). The success of the comparisons between experiment and theoretical predictions for the cases considered may be improved by inclusion of other factors in the present model, as discussed in the following section.

Table 1 Tabulated data for each icing encounter (Ref. 7)

Encounter Number	Time of buildup, MST	Average propeller speed during buildup, rpm	Blade angle at 0.75R during efficiency measurement	Average pressure altitude during ice buildup, ft	Average true airspeed during ice buildup, mph	Free air temperature, °F	Average liquid water content, g/m^3	Maximum liquid water content, g/m^3	Average droplet diameter, μ	Average icing rate, in./h
2	1513 – 1523	1025	31.8	10,000	158	1	0.41	1.0	18	6.1
4	1512 – 1521	1025	31.8	9,200	155	3	0.44	1.18	25	6.3
9	1500 – 1502	1025	21.5	15,200	178	−6	0.10	0.24	27	1.6
11	1515 – 1540	1025	29.5	12,000	155	3	0.28	0.73	35	4.1
12	1402 – 1435	1175	28.0	22,700	178	−22	0.14	0.39	14	2.3

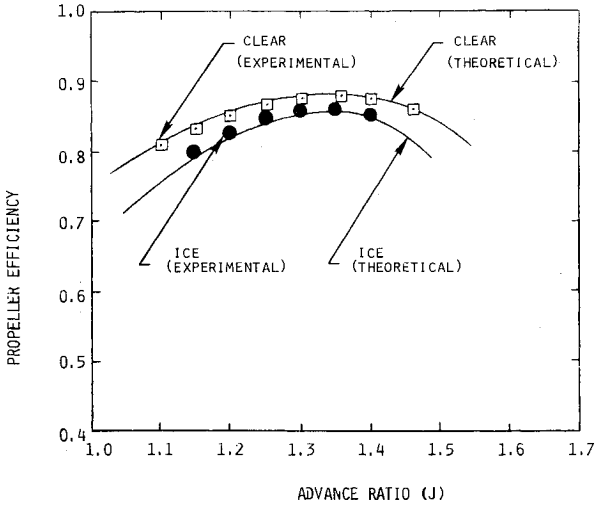

Fig. 10 Comparison between theoretical/experimental η values — encounter 2 (Ref. 7).

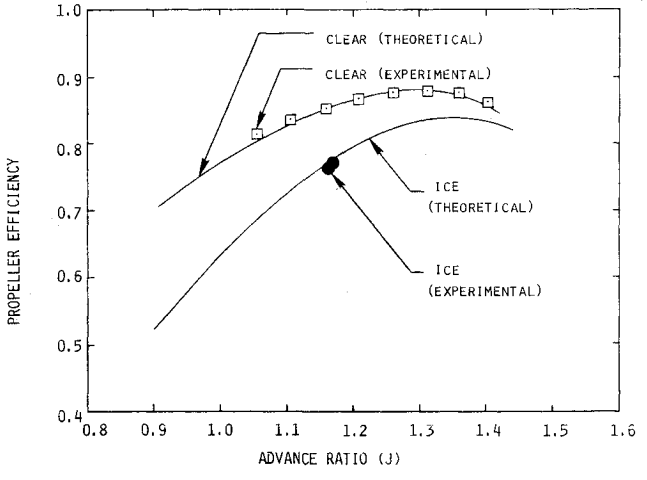

Fig. 11 Comparison between theoretical/experimental η values — encounter 4 (Ref. 7).

Current Methodology Refinements

The present analytical model of ice accretion, although providing reasonable values of performance degradation for rotating systems, can be further refined by the inclusion of additional elements. For example:

1) Consideration of the decambering effect due to ice accretion at the leading edge of the airfoil, leading to a shift in the zero lift angle of attack.

2) The reduction of the maximum lift coefficient due to ice accretion.

3) Inclusion of appropriate centrifugal/adhesion force models, using as a base the results of Loughborough and Haas[15] and the influence of kinetic heating and its relationship to the adhesion model.

4) The unsteady effects on airfoil performance under the influence of ice accretion.

5) Re-examination of the drag coefficient correlation for both the rime and glaze ice condition.

6) Consideration of ice shedding, both symmetrical and asymmetrical, leading to adverse vibration.

7) Airfoil design capability to minimize the ice accretion process for propeller systems.

Work has been initiated in these areas. As progress is made, the current methodology will be updated to provide a more complete modeling of the ice accretion process for rotating systems.

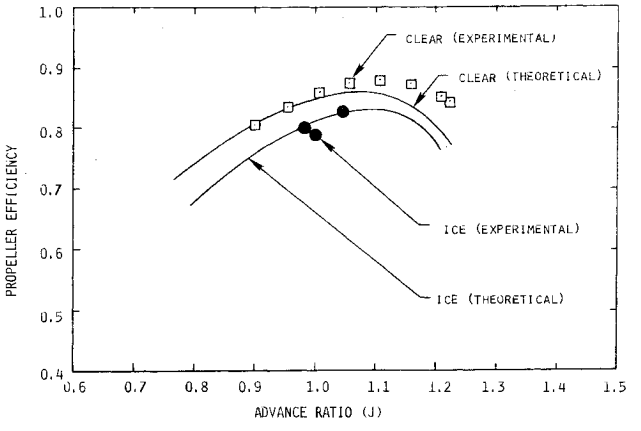

Fig. 12 Comparison between theoretical/experimental η values—encounter 12 (Ref. 7).

Summary

The present analytical model provides the means to assess performance degradation due to ice accretion on propeller configurations and yields changes in performance levels that compare well with available experimental data. However, additional theoretical/experimental comparisons are needed for the propeller case. Refinements to the present analytical model have been suggested and will be included as the current study progresses.

Acknowledgment

The authors wish to acknowledge the support of the NASA Lewis Research Center, under Grants NAG 3-109 and NAG 3-242, for the research contained in the paper.

References

[1]Rodert, L. A., "The Effects of Aerodynamic Heating on Ice Formations on Airplane Propellers," NACA TN-799, March 1941.

[2]Corson, B. W. Jr., and Maynard, J. D., "Investigation of the Effect of a Tip Modification and Thermal De-Icing Air Flow on Propeller Performance," NACA TN-1111, July 1946.

[3]Corson, B. S., Jr., and Maynard, J. D., "Analysis of Propeller Efficiency Losses Associated with Heated-Air Thermal De-Icing," NACA TN-1112, July 1946.

[4]Darsow, J. F., and Selna, J., "A Flight Investigation of the Thermal Performance of an Air Heated Propeller," NACA TN-1178, April 1947.

[5]Gray, V. H. and Campbell, R. G., "A Method for Estimating Heat Requirements for Ice Prevention on Gas-Heated Hollow Propeller Blades," NACA TN-1494, Dec. 1947.

[6]Preston, C. M. and Blackman, C. D., "Effects of Ice Formations on Airplane Performance in Level Cruise Flight," NACA TN-1598, May 1948.

[7]Neel, C. B. Jr., and Bright, L. G., "The Effect of Ice Formation on Propeller Performance," NACA TN-2212, Oct. 1950.

[8]Sweet, D., Private Communication, B. F. Goodrich Co., Akron, Ohio, 1980.

[9]O'Connor, M., Private Communication, Gulfstream Aerospace Corporation, Bethany, Okla., 1981.

[10]Bragg, M. B., Gregorek, G. M., and Shaw, R. J. "An Analytical Approach to Airfoil Icing," AIAA Paper 81-0403, Jan. 1981.

[11]Bragg, M. B. and Gregorek, G. M., "Aerodynamic Characteristics of Airfoils with Ice Accretions," AIAA Paper 82-0282, Jan. 1982.

[12]Cooper, J. P., "The Linearized Inflow Propeller Strip Analysis," Wright Air Development Center, Wright-Patterson AFB, Ohio, WADC TR 56-615, Feb. 1957.

[13]Korkan, K. D. and Gregorek, G. M., "Propeller Aeroacoustic Methodologies," NASA CP-2126, Nov. 1979.

[14]Korkan, D. D., Gregorek, G. M., and Mikkelson, D. C., "A Theoretical and Experimental Investigation of Propeller Performance Methodologies," AIAA Paper 80-1240, June 1980.

[15]Loughborough, D. L. and Haas, E. G., "Reduction of the Adhesion of Ice to De-Icer Surfaces," *Journal of Aerospace Science*, Vol. 13, March 1946, pp. 126-134.